

## Supplementary Information

Electronic structure modulation of bismuth catalysts induced by sulfur  
and oxygen co-doping for promoting CO<sub>2</sub> electroreduction

Xiaolin Shao<sup>a</sup>, Xueliang Sun<sup>a</sup>, Qiuhan Huang<sup>a</sup>, Jin Yi<sup>a</sup>, Jiujun Zhang<sup>a</sup> and Yuyu Liu<sup>a,\*</sup>

<sup>a</sup> Department of Chemistry/Institute for Sustainable Energy, College of Sciences, Shanghai  
University, Shangda Road 99, Baoshan, Shanghai 200444, China.

\*Corresponding authors: E-mail addresses: liuyuyu@shu.edu.cn (Yuyu Liu).

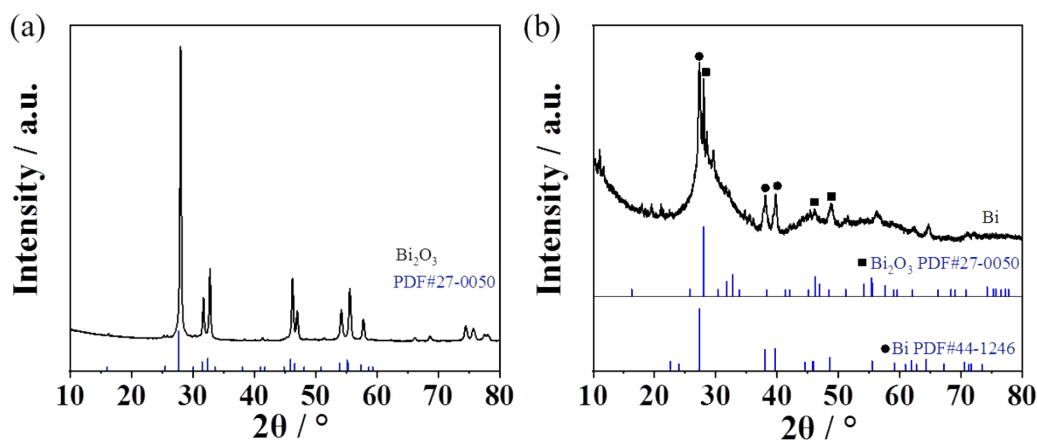


Fig. S1 XRD patterns of (a)  $\text{Bi}_2\text{O}_3$  and (b) Bi.

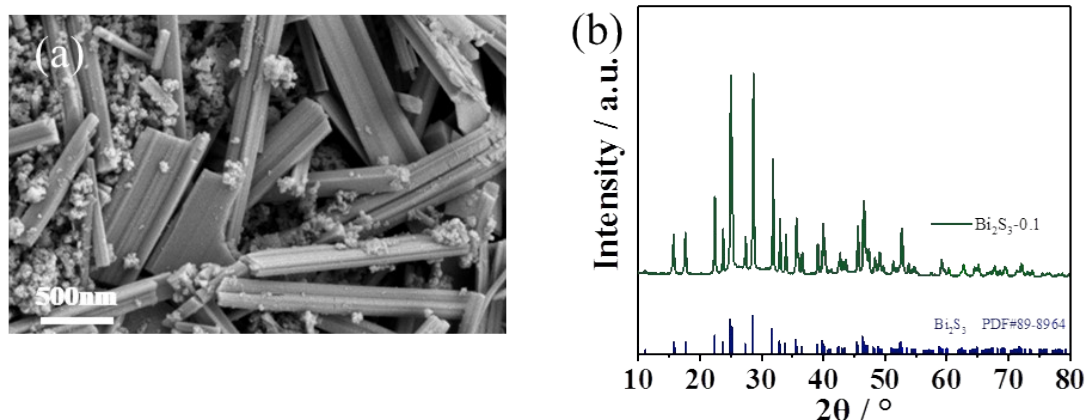


Fig. S2 (a) SEM image and (b) XRD pattern of  $\text{Bi}_2\text{S}_3$ -0.1.

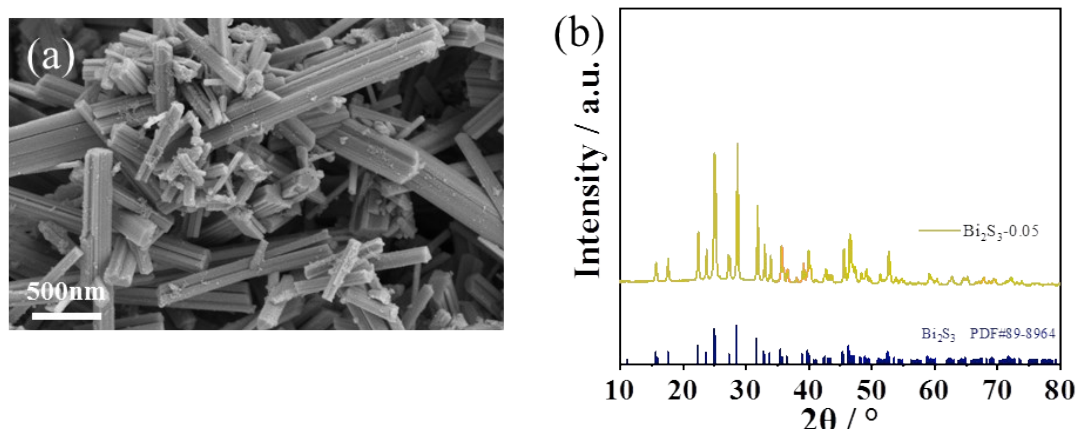


Fig. S3 (a) SEM image and (b) XRD pattern of  $\text{Bi}_2\text{S}_3\text{-}0.05$ .

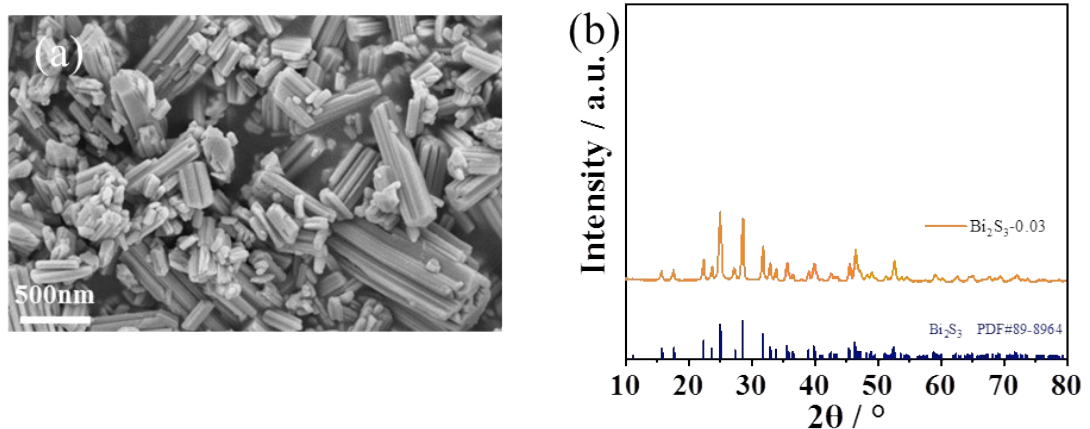


Fig. S4 (a) SEM image and (b) XRD pattern of  $\text{Bi}_2\text{S}_3\text{-}0.03$ .

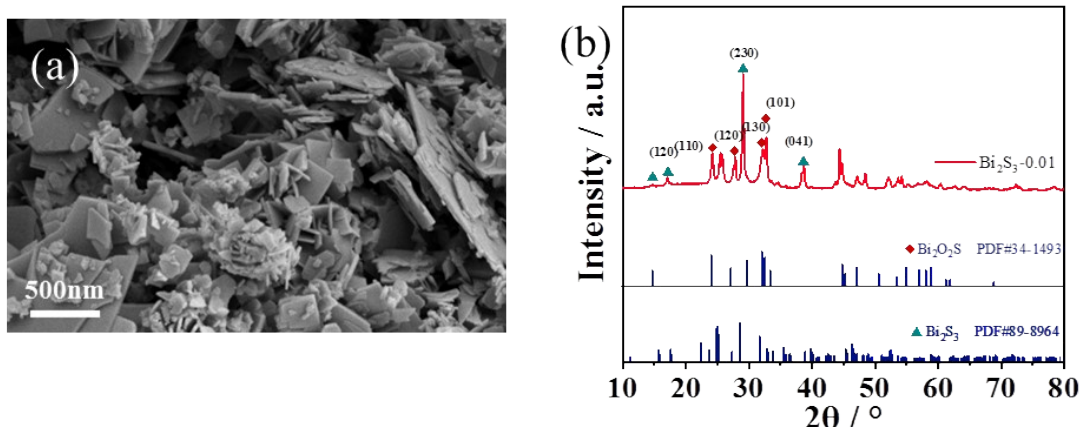


Fig. S5 (a) SEM image and (b) XRD pattern of  $\text{Bi}_2\text{S}_3$ -0.01.

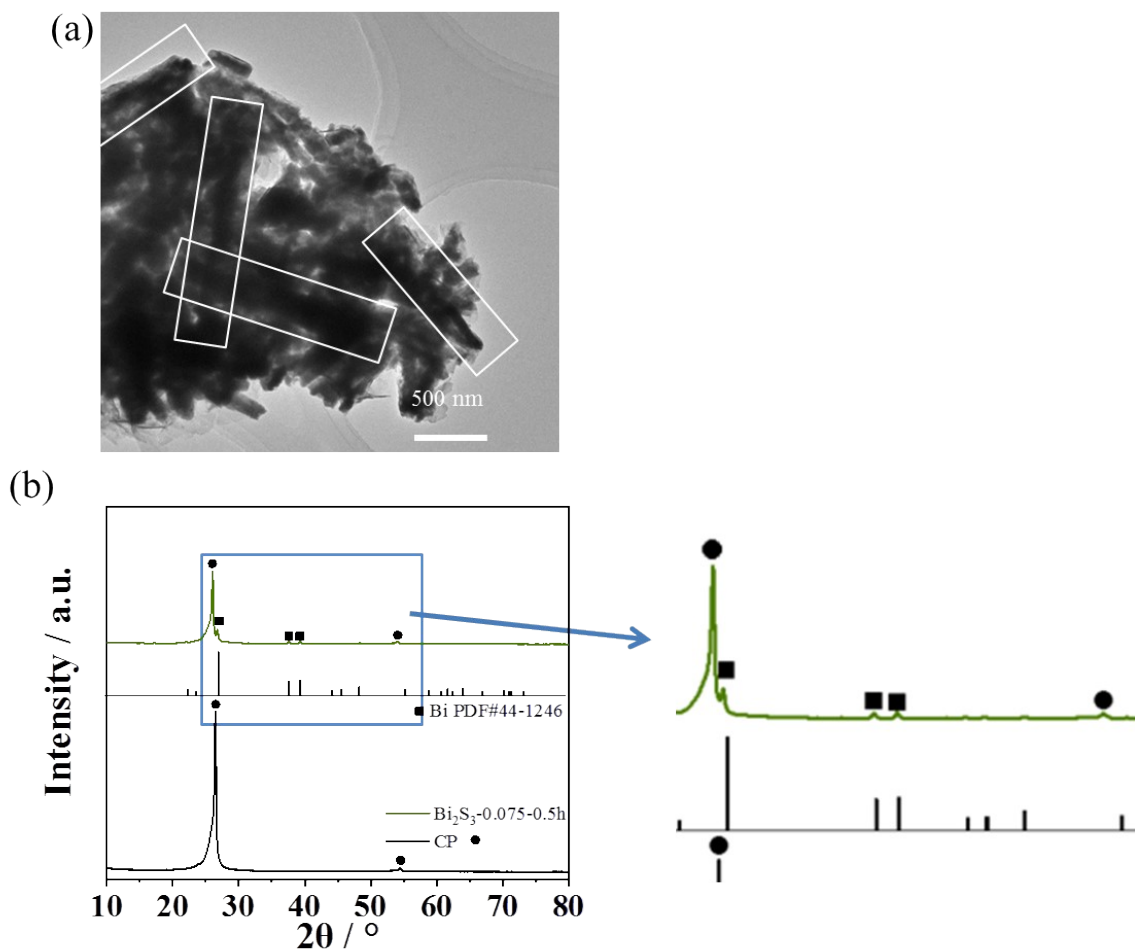


Fig. S6 (a) TEM image of  $\text{Bi}_2\text{S}_3$ -0.075-D-0.5h, (b) XRD patterns of  $\text{Bi}_2\text{S}_3$ -0.075-D-0.5h and CP.

In Fig. S6(a), because the material was scraped off the carbon paper after the reaction, some carbon paper debris was mixed.

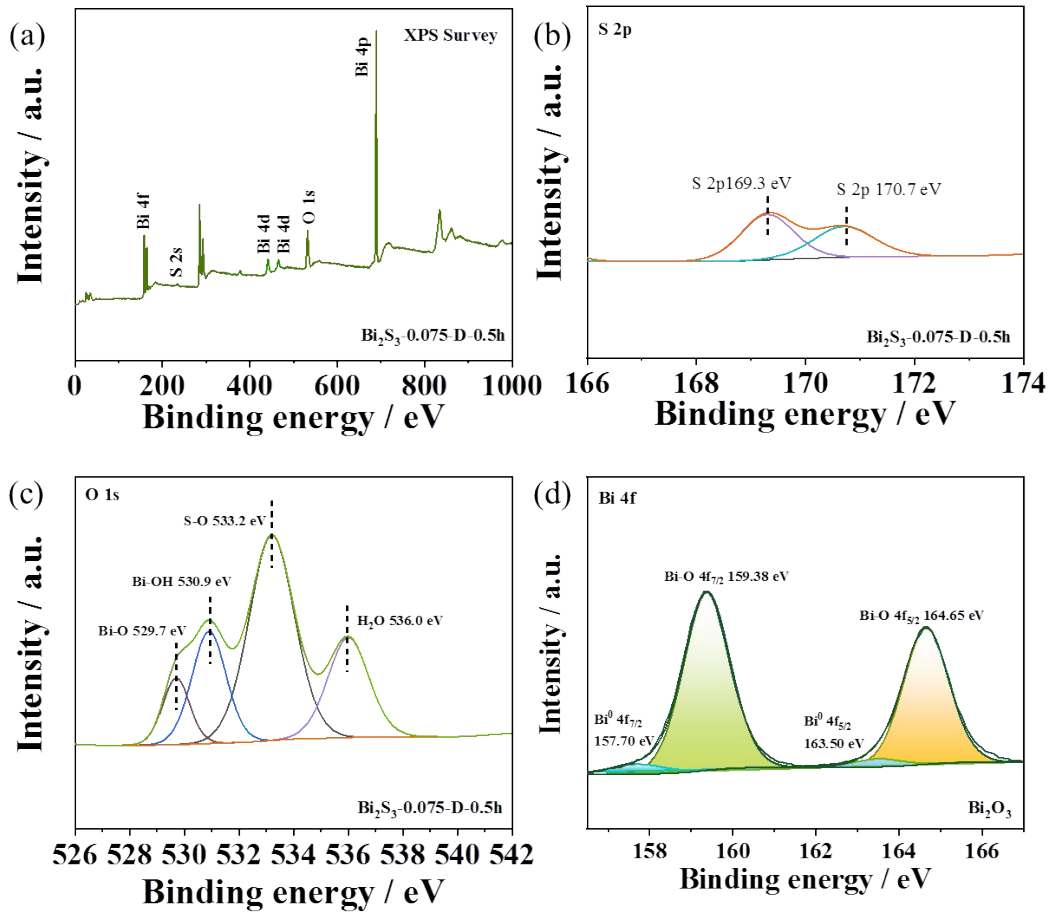


Fig. S7 XPS survey spectra of (a)  $\text{Bi}_2\text{S}_3$ -0.075-D-0.5h, (b) S 2p, (c) O 1s of  $\text{Bi}_2\text{S}_3$ -0.075-D-0.5h electrode and (d) Bi 4f of  $\text{Bi}_2\text{O}_3$  derived electrode.

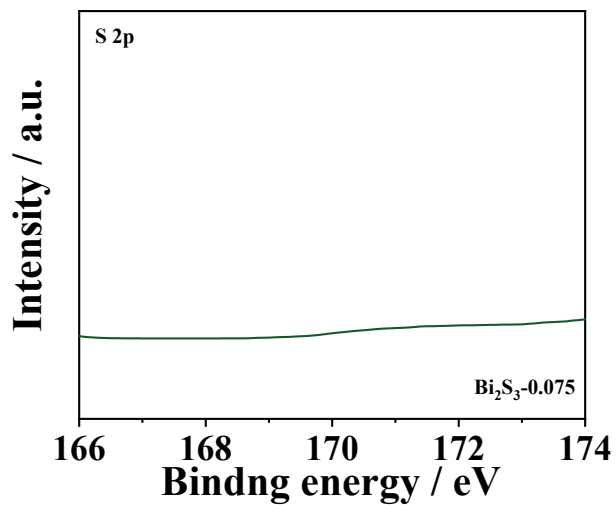


Fig. S8 XPS survey spectra of S 2p of  $\text{Bi}_2\text{S}_3$ -0.075 electrode.

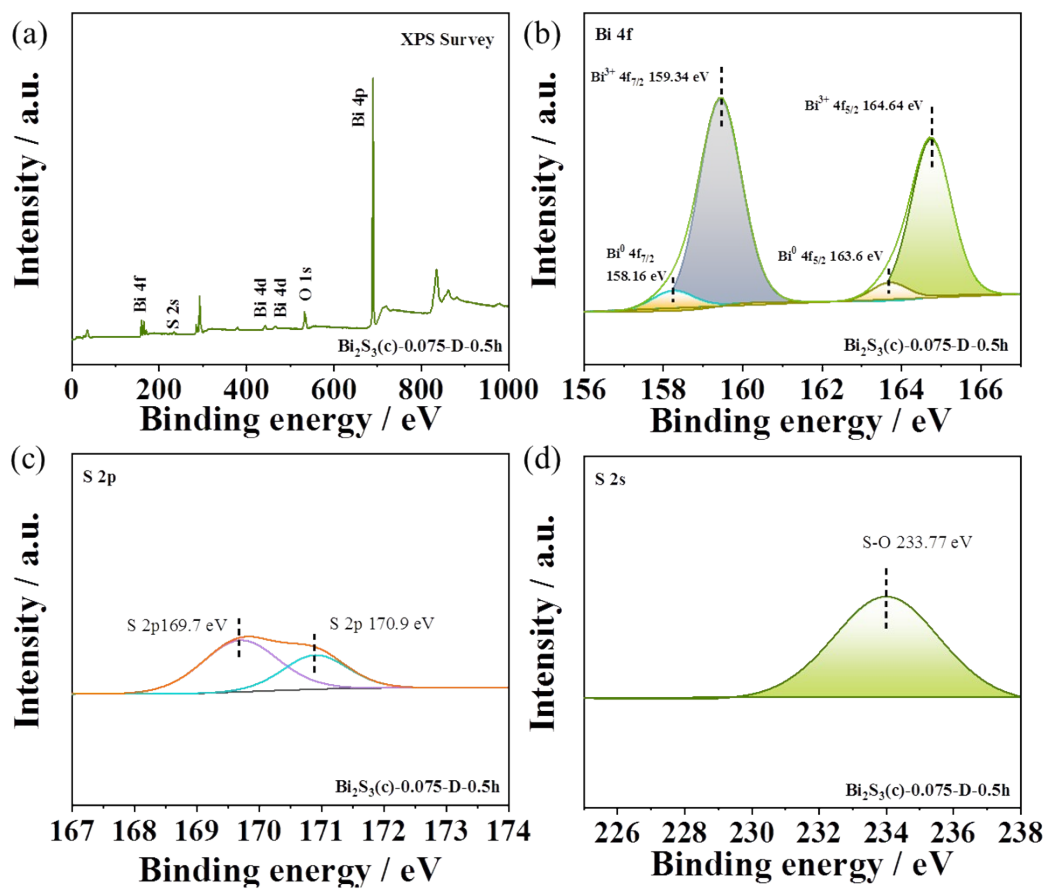


Fig. S9 XPS survey spectra of (a)  $\text{Bi}_2\text{S}_3(\text{c})\text{-}0.075\text{-D-}0.5\text{h}$  and (b) Bi 4f, (c) S 2p and (d) S 2s of  $\text{Bi}_2\text{S}_3(\text{c})\text{-}0.075\text{-D-}0.5\text{h}$  electrode.

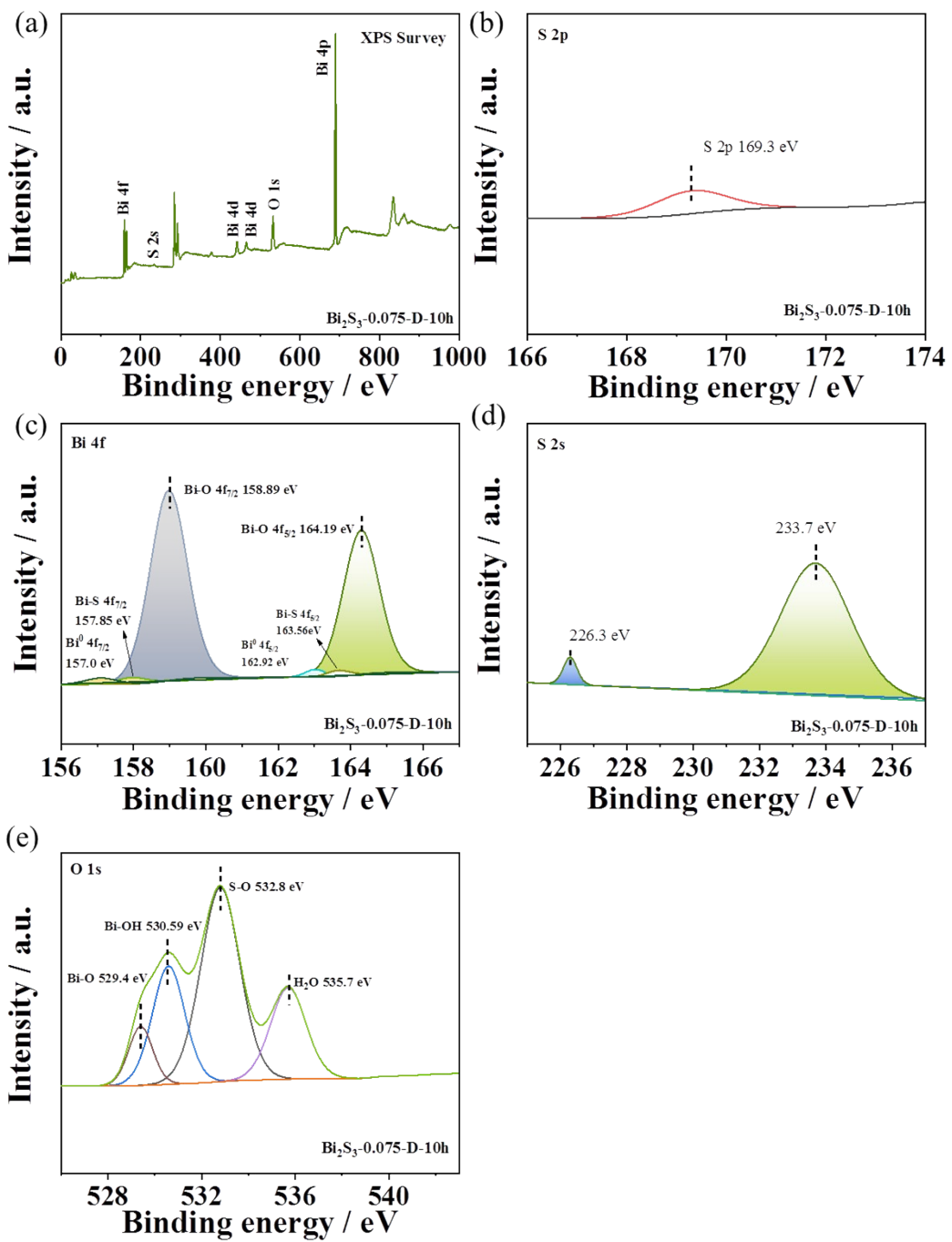


Fig. S10 XPS survey spectra of (a)  $\text{Bi}_2\text{S}_3\text{-}0.075\text{-D-}10\text{h}$  and (b) Bi 4f, (c) S 2p, (d) S 2s and (e) O 1s of  $\text{Bi}_2\text{S}_3\text{-}0.075\text{-D-}10\text{h}$  electrode.

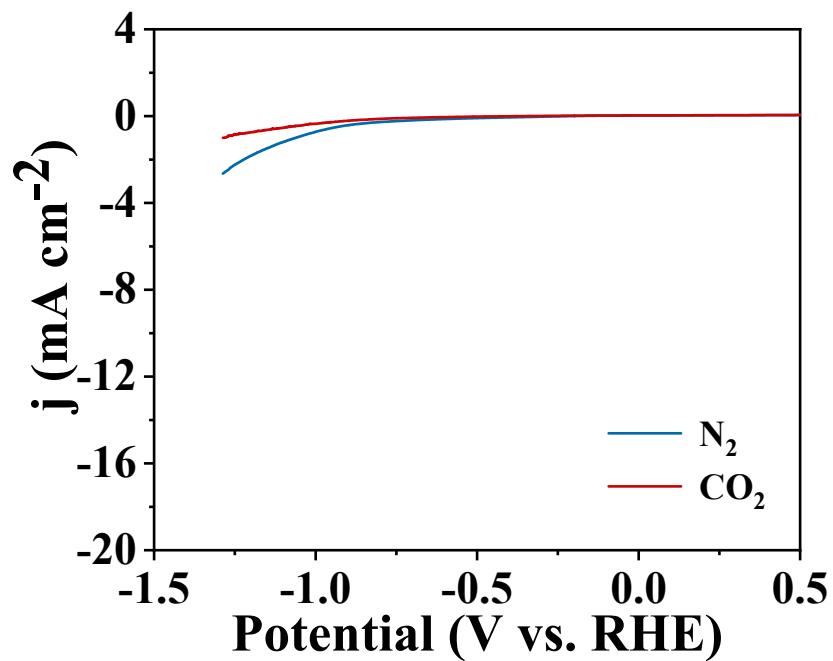


Fig. S11 LSV curves of CP in  $\text{N}_2$  and  $\text{CO}_2$  atmosphere in 0.1 M  $\text{KHCO}_3$  at  $50 \text{ mV s}^{-2}$ .

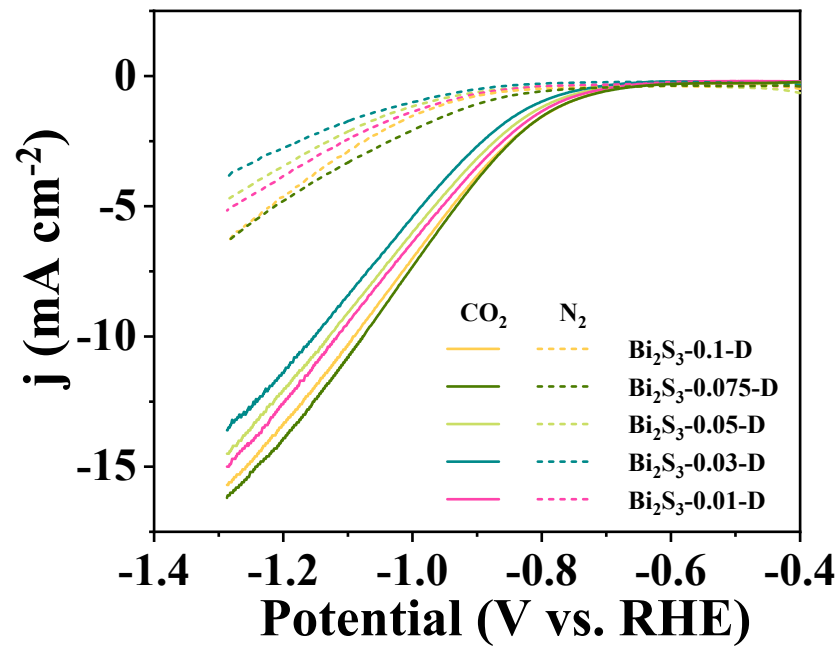


Fig. S12 LSV curves of  $\text{Bi}_2\text{S}_3$ -0.1-D,  $\text{Bi}_2\text{S}_3$ -0.075-D,  $\text{Bi}_2\text{S}_3$ -0.05-D,  $\text{Bi}_2\text{S}_3$ -0.03-D to  $\text{Bi}_2\text{S}_3$ -0.01-D in  $\text{N}_2$ -saturated and  $\text{CO}_2$ -saturated 0.1 M  $\text{KHCO}_3$  at  $50 \text{ mV s}^{-2}$ .

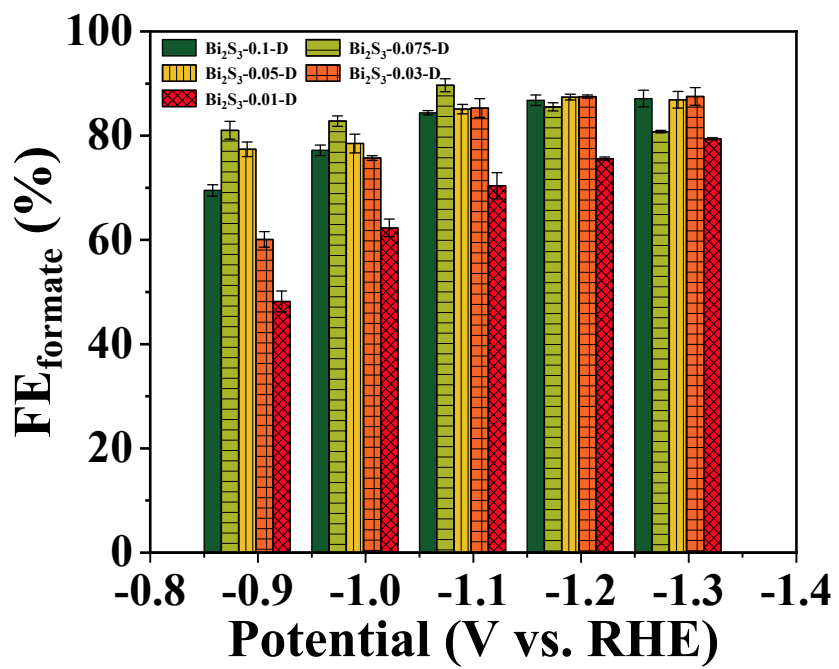


Fig. S13 The FE<sub>formate</sub> of Bi<sub>2</sub>S<sub>3</sub>-0.1-D, Bi<sub>2</sub>S<sub>3</sub>-0.075-D, Bi<sub>2</sub>S<sub>3</sub>-0.05-D, Bi<sub>2</sub>S<sub>3</sub>-0.03-D and Bi<sub>2</sub>S<sub>3</sub>-0.01-D electrodes at different applied potential.

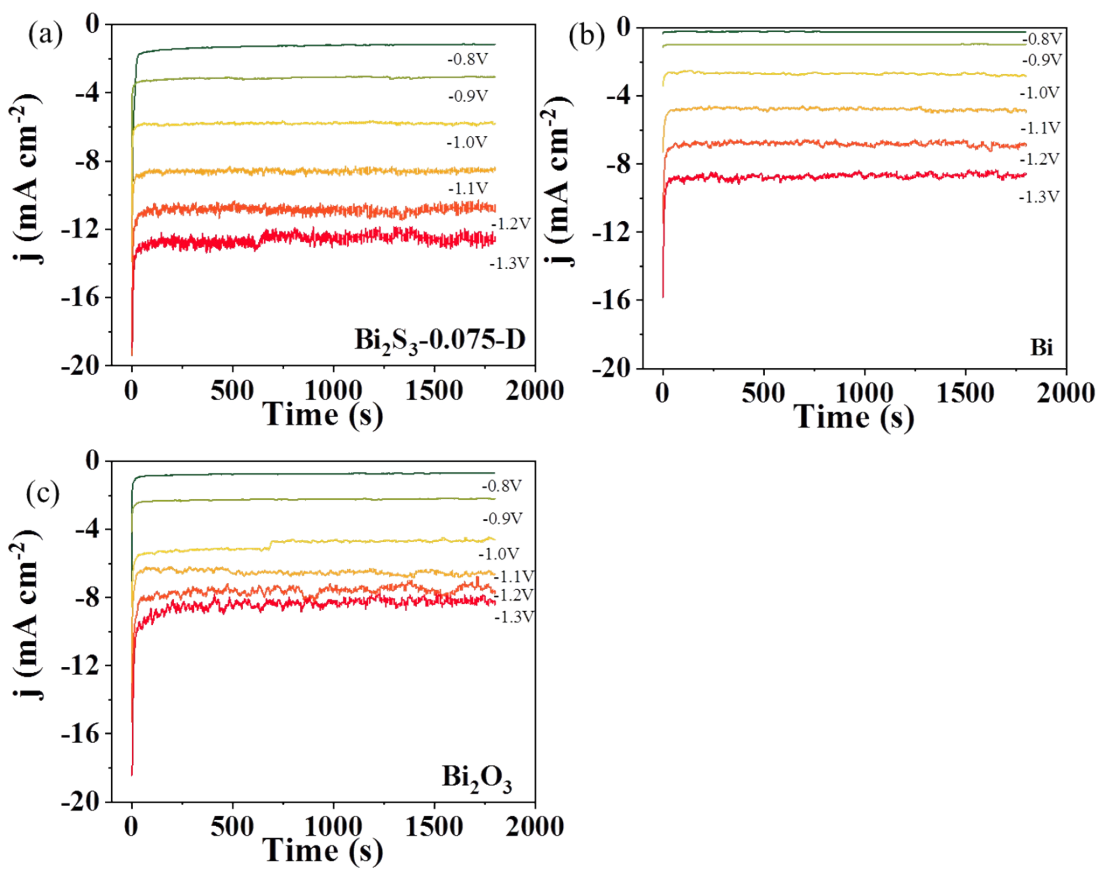


Fig. S14 I-t curves of ERCO<sub>2</sub> over (a)  $\text{Bi}_2\text{S}_3\text{-}0.075\text{-D}$ , (b) Bi and (d)  $\text{Bi}_2\text{O}_3$  at different potential within 1800 s.

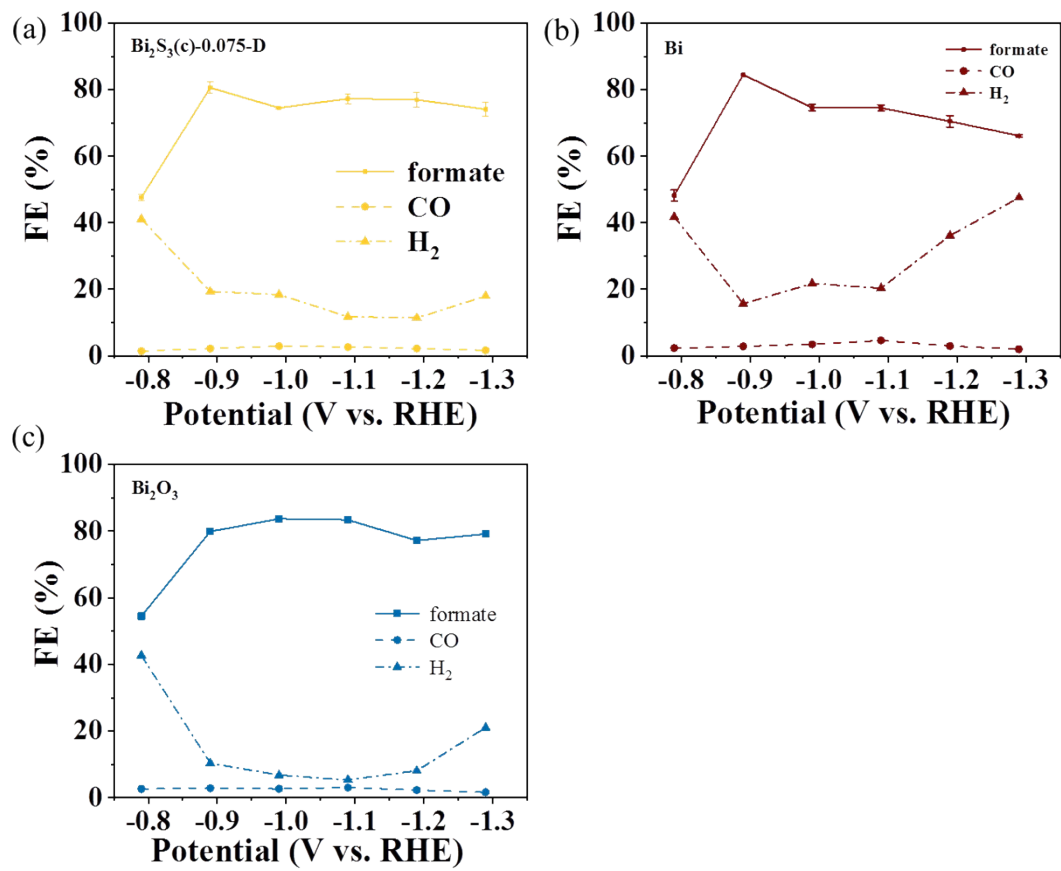


Fig. S15 FE of formate, CO and H<sub>2</sub> over (a) Bi<sub>2</sub>S<sub>3</sub>(c)-0.075-D, (b) Bi and (c) Bi<sub>2</sub>O<sub>3</sub> electrodes.

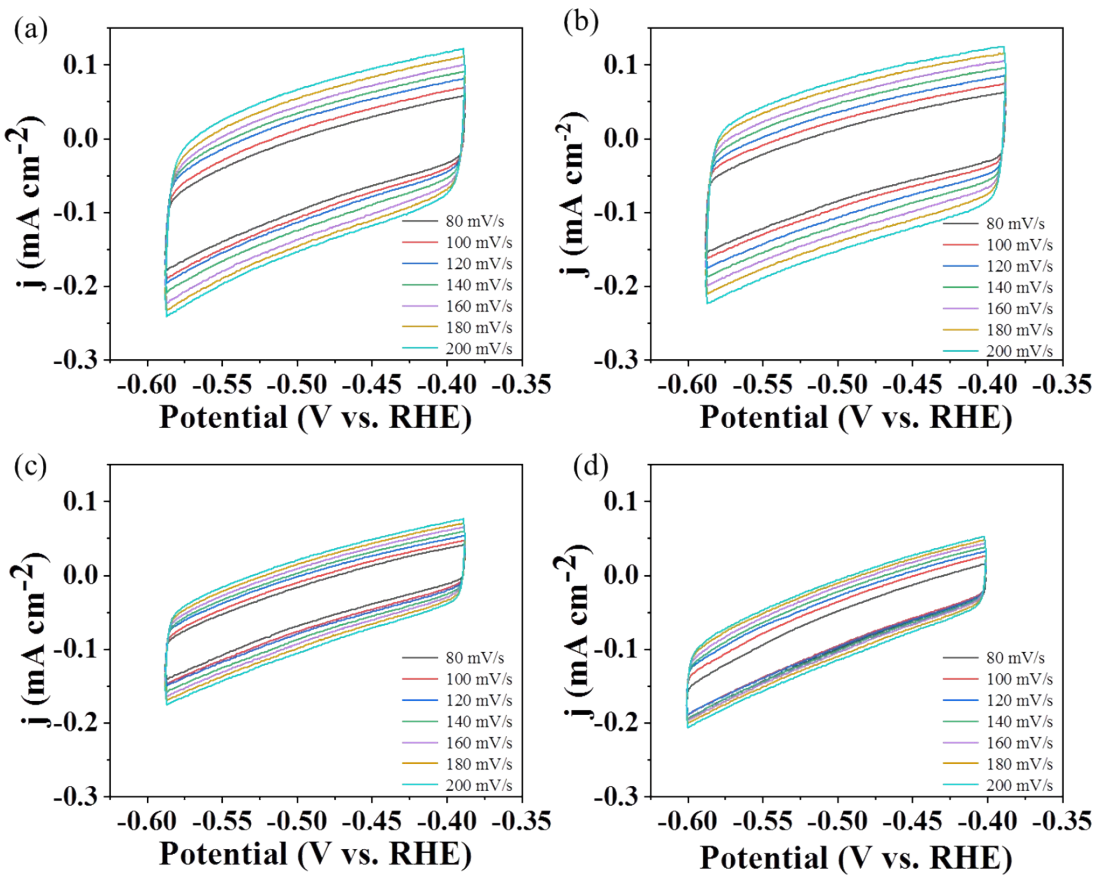


Fig. S16 CV curves of (a)  $\text{Bi}_2\text{S}_3\text{-}0.1\text{-D}$ , (b)  $\text{Bi}_2\text{S}_3\text{-}0.075\text{-D}$ , (c)  $\text{Bi}_2\text{S}_3\text{-}0.05\text{-D}$  and (d)  $\text{Bi}_2\text{S}_3\text{-}0.03\text{-D}$  at the range of  $-0.4$  to  $-0.6$  V with different scan rates in  $\text{N}_2$ -saturated 0.1 M  $\text{KHCO}_3$  solution.

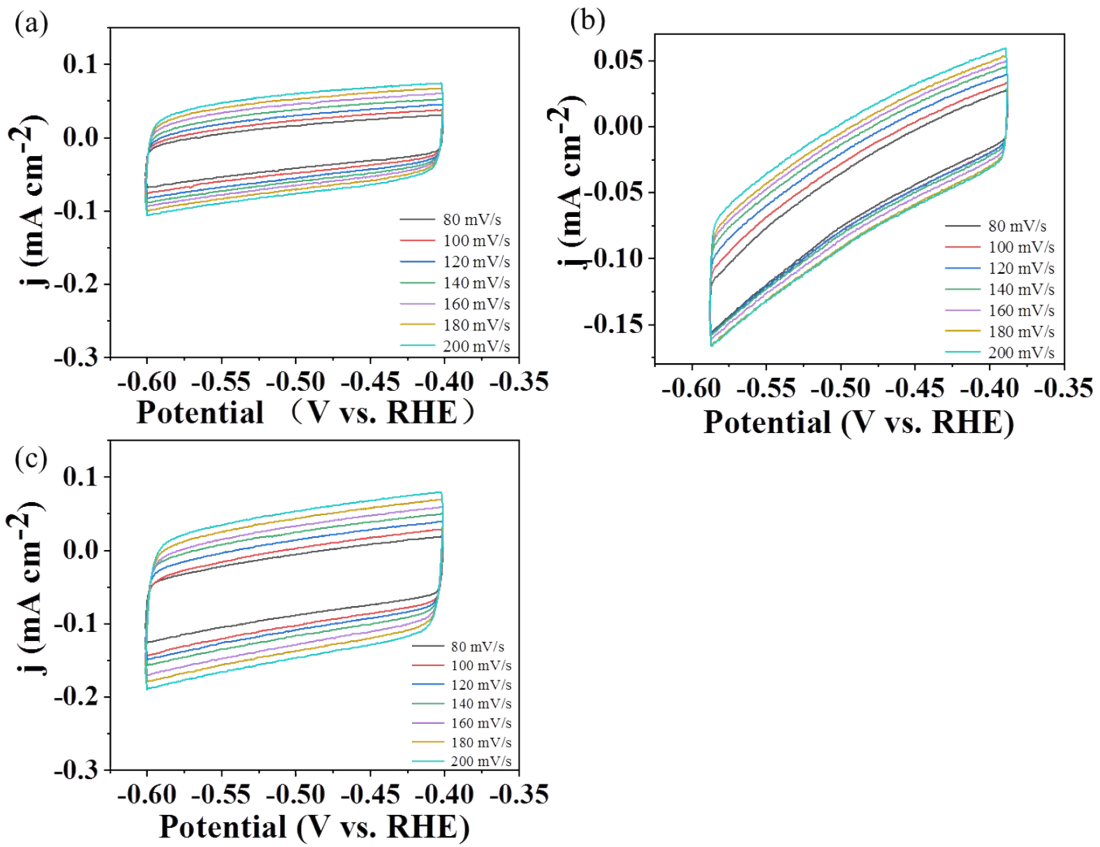


Fig. S17 CV curves of (a) Bi, (b) Bi<sub>2</sub>S<sub>3</sub>(c)-0.075-D and (c) Bi<sub>2</sub>O<sub>3</sub> at the range of -0.4 to -0.6 V with different scan rates in N<sub>2</sub>-saturated 0.1 M KHCO<sub>3</sub> solution.

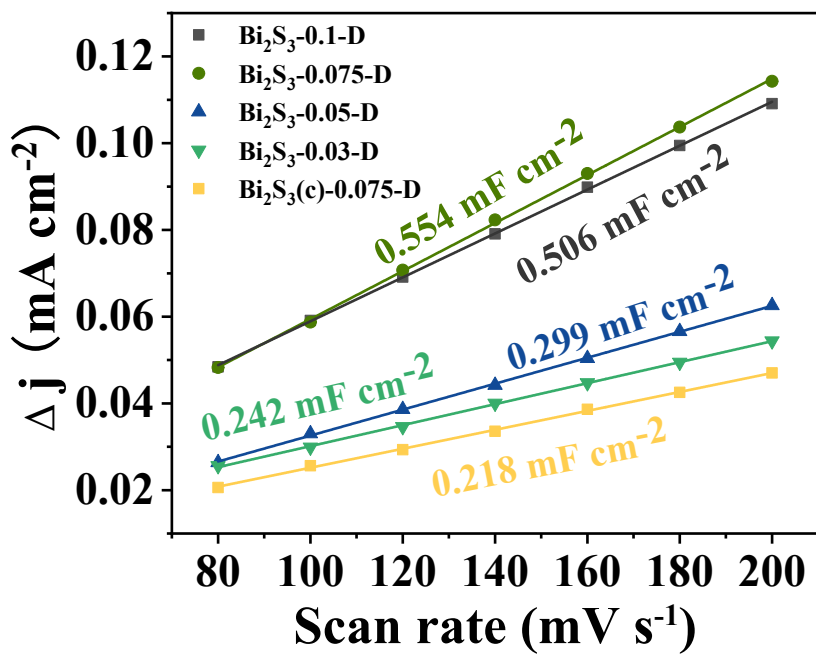


Fig. S18 Comparison of corresponding Cdl of  $\text{Bi}_2\text{S}_3\text{-}0.1\text{-D}$ ,  $\text{Bi}_2\text{S}_3\text{-}0.075\text{-D}$ ,  $\text{Bi}_2\text{S}_3\text{-}0.05\text{-D}$  and  $\text{Bi}_2\text{S}_3\text{-}0.03\text{-D}$  samples.

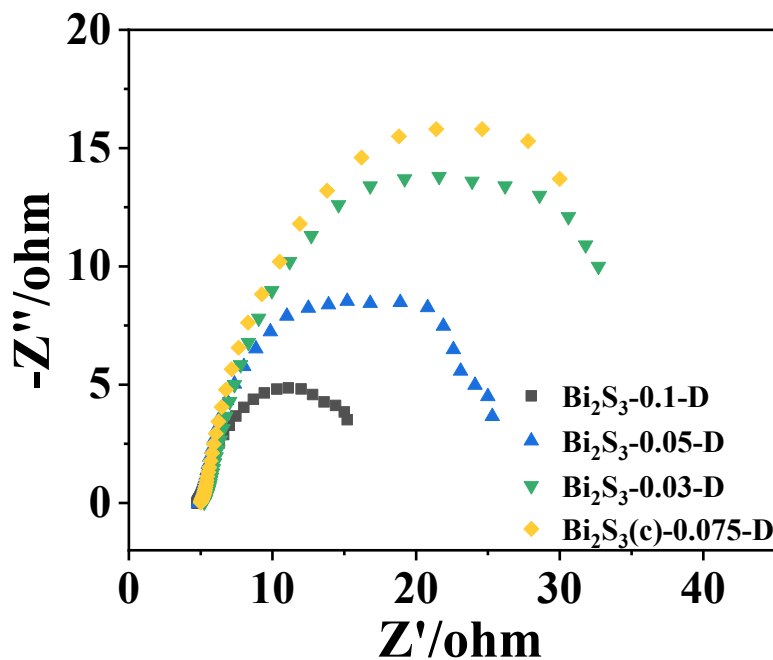


Fig. S19 EIS measurements of  $\text{Bi}_2\text{S}_3\text{-}0.1\text{-D}$ ,  $\text{Bi}_2\text{S}_3\text{-}0.075\text{-D}$ ,  $\text{Bi}_2\text{S}_3\text{-}0.05\text{-D}$  and  $\text{Bi}_2\text{S}_3\text{-}0.03\text{-D}$  samples at the potential of  $-1.09\text{V}_{\text{RHE}}$ .

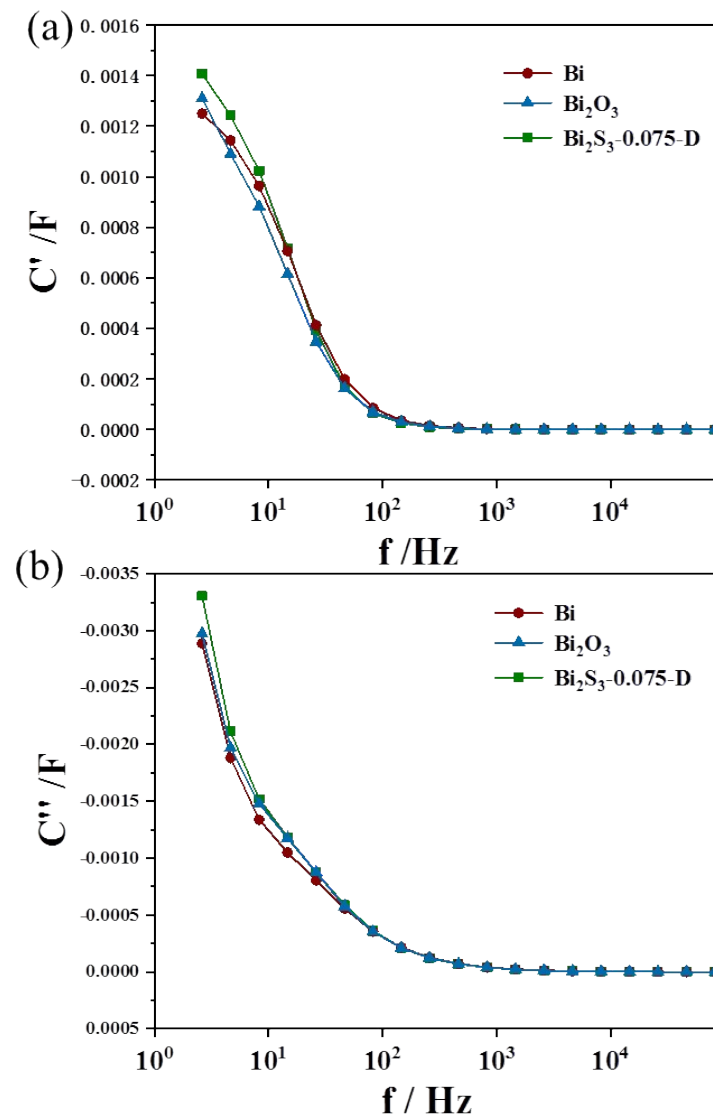


Fig. S20 Bode plots of (a) real part and (b) imaginary part of complex capacitance with respect to frequency of  $\text{Bi}_2\text{S}_3\text{-}0.075\text{-D}$ ,  $\text{Bi}_2\text{O}_3$  and  $\text{Bi}$  samples.

Sample	Bi : S: O (atomic rate)
Bi <sub>2</sub> S <sub>3</sub>	1:1.47
Bi <sub>2</sub> S <sub>3</sub> -0.075-D-0.5h	1:10.24:11.28
Bi <sub>2</sub> S <sub>3</sub> (c)-0.075-D-0.5h	1:20.87:6.76
Bi <sub>2</sub> S <sub>3</sub> -0.075-D-10h	1:10.09:10.35

Table S1 Atomic ratio of Bi to S in different materials.

Catalysts	Bi <sub>2</sub> S <sub>3</sub>	Bi <sub>2</sub> S <sub>3</sub> -0.075-D-0.5h	Bi <sub>2</sub> S <sub>3</sub> (c)-0.075-D-0.5h	Bi <sub>2</sub> S <sub>3</sub> -0.075-D-10h	Bi <sub>2</sub> O <sub>3</sub> -D
A	574912.	2536.52	-	1466.67	-
Bi3+	88				
4f7/2(Bi2S3)					
A	424810.	1903.91	-	1052.90	-
Bi3+	24				
4f5/2(Bi2S3)					
A	-	19328.47	30788.72	54715.12	65338.93
Bi3+					
4f7/2(Bi2O3)					
A	-	14291.91	22414.77	40026.79	48735.22
Bi3+					
4f5/2(Bi2O3)					
A	-	2119.97	3091.30	1582.9	4331.67
Bi0 4f7/2					
A	-	1571.28	2373.81	1194.17	3124.51
Bi0 4f5/2					

Table S2 Peak area parameters of XPS spectrum for Bi 4f of different catalysts.

Catalysts	ECSA(cm <sup>2</sup> )
Bi <sub>2</sub> S <sub>3</sub> -0.075	6.925
Bi	4.06
Bi <sub>2</sub> O <sub>3</sub>	6.05

Table S3 The electrochemical active surface area of different catalysts.

Catalyst	Electrolyte	Potential (V vs. RHE)	J (mA cm <sup>-2</sup> )	FE <sub>formate</sub> (%)	Ref.
Defect-rich Bi (derived from Bi <sub>2</sub> S <sub>3</sub> )	0.5 M NaHCO <sub>3</sub>	−0.75	5	84	<sup>1</sup>
Bi with rich Bi-O bond (derived from Bi <sub>2</sub> S <sub>3</sub> )	0.5 M KHCO <sub>3</sub>	−1.0	6.6	80	<sup>2</sup>
Bi <sub>2</sub> S <sub>3</sub> - Bi <sub>2</sub> O <sub>3</sub> @rGO	0.1 M KHCO <sub>3</sub>	−0.9	4	90.1	<sup>3</sup>
S doped BiOC	0.5 M KHCO <sub>3</sub>	−0.9	30	96.7	<sup>4</sup>
Bi nanoparticles	0.5 M KHCO <sub>3</sub>	−0.83	55	86	<sup>5</sup>
β-Bi <sub>2</sub> O <sub>3</sub>	0.1 M KHCO <sub>3</sub>	−1.2	20.9	87	<sup>6</sup>
Bi nanosheets	0.1 M KHCO <sub>3</sub> (flow cell)	−1.36	210	88.1	<sup>7</sup>
Bi/Bi <sub>2</sub> O <sub>3</sub> nanoparticles	0.5 M KHCO <sub>3</sub>	−0.9	18	85	<sup>8</sup>
Bi Dendrite	0.5 M KHCO <sub>3</sub>	−0.74	3.2	89	<sup>9</sup>
Bi nanosheets	0.1 M KHCO <sub>3</sub>	−1.1	17	86.0	<sup>10</sup>
S and O co- doping Bi	0.1 M KHCO <sub>3</sub>	−1.09	9	89.7	This work

Table S4 The performance of CO<sub>2</sub> electroreduction to formate over Bi-based catalysts reported recently.

## References

1. Y. Zhang, F. W. Li, X. L. Zhang, T. Williams, C. D. Easton, A. M. Bond and J. Zhang, *J. Mater. Chem. A*, 2018, **6**, 4714-4720.
2. Y. T. Wang, L. Cheng, J. Z. Liu, C. Q. Xiao, B. Zhang, Q. H. Xiong, T. Zhang, Z. L. Jiang, H. Jiang, Y. H. Zhu, Y. H. Li and C. Z. Li, *Chelectrochem*, 2020, **7**, 2864-2868.
3. X. Yang, P. Deng, D. Liu, S. Zhao, D. Li, H. Wu, Y. Ma, B. Y. Xia, M. Li, C. Xiao and S. Ding, *J. Mater. Chem. A*, 2020, **8**, 2472-2480.
4. J. Wang, J. Mao, X. Zheng, Y. Zhou and Q. Xu, *Appl. Surf. Sci.*, 2021, **562**, 150197.
5. W. Dan, W. Xuewan, F. Xian-Zhu and L. Jing-Li, *Appl. Catal. B-Environ.*, 2021, **284**, 119723.
6. T.-P. Thanh, R. Daiyan, Z. Fusco, Z. Ma, R. Amal and A. Tricoli, *Adv. Funct. Mater.*, 2020, **30**, 1906478.
7. J. Yang, X. L. Wang, Y. T. Qu, X. Wang, H. Huo, Q. K. Fan, J. Wang, L. M. Yang and Y. E. Wu, *Adv. Energy Mater.*, 2020, **10**, 2001709.
8. J. J. Sun, W. Z. Zheng, S. L. Lyu, F. He, B. Yang, Z. J. Li, L. C. Lei and Y. Hou, *Chin. Chem. Lett.*, 2020, **31**, 1415-1421.
9. J. H. Koh, D. H. Won, T. Eom, N. K. Kim, K. D. Jung, H. Kim, Y. J. Hwang and B. K. Min, *ACS Catal.*, 2017, **7**, 5071-5077.
10. W. Zhang, Y. Hu, L. Ma, G. Zhu, P. Zhao, X. Xue, R. Chen, S. Yang, J. Ma, J. Liu and Z. Jin, *Nano Energy*, 2018, **53**, 808-816.